ELSEVIER

Journal of Hazardous Materials A89 (2002) 127–139

Journal of Hazardous Materials

www.elsevier.com/locate/jhazmat

Surface tension prediction for hydrocarbons and its application to level swell modelling

Peter Cumber*

Department of Mechanical and Chemical Engineering, Heriot Watt University, Edinburgh EH14 4AS, UK

Received 21 May 2001; received in revised form 7 September 2001; accepted 17 September 2001

Abstract

In this article, methods for estimating surface tension are considered where the specific gravity and normal boiling point are known such as when the composition is expressed using petroleum fractions. This is of interest as surface tension is an important parameter in the calculation of outflow conditions from a two-phase vessel undergoing level swell. A new improved correlation for the parachor is presented and the improved accuracy of the surface tension and bubble rise velocity compared to when the original parachor correlation is used is assessed.

Finally the sensitivity of outflow predictions to changes in the surface tension is presented for a depressurising vessel containing pentane. For the vessel depressurisation simulation where the original parachor correlation is used, two-phase venting is maintained for two–three times as long compared to when the actual parachor or improved parachor correlation is used to estimate the surface tension. This has an impact on the error in predicting the mass flow rate as a source condition for other consequence models and also in vent sizing calculations.

Keywords: Surface tension; Level swell; Vessel outflow; Petroleum fractions; Emergency pressure relief

1. Introduction

The storage and processing of fluids in a two-phase state at pressure requires the consequences of a failure of the vessel wall or a pipe break due to corrosion or third party interference be considered, as part of a safety analysis. In this article, methods for estimating surface tension and associated quantities are considered, where the specific gravity and normal boiling point are known, such as when the composition is expressed using petroleum

* Tel.: +44-131-451-3532.
E-mail address: p.s.cumber@hw.ac.uk (P. Cumber).

0304-3894/02/$ – see front matter
PII: S0304-3894(01)00354-5

Nomenclature

A_{vent}	vent area
$A_{ves,cros}$	cross-sectional area of the vessel
$\tilde{E}_{rel}$	relative error
g	gravitational constant
j_L	liquid phase superficial velocity
j_G	gas phase superficial velocity
M_H	hydrogen content
M_w	molecular weight
N	atomicity
N_ν	parameter in the bubble rise velocity correlation in Eq. (4)
$[P]$	parachor
U_{bub}	bubble rise velocity
U_L	area averaged liquid phase velocity
U_G	area averaged gas phase velocity
x_q	stagnation vapour quality

Greek characters

ν_f	vessel void fraction
ν_L	kinematic viscosity of the liquid phase
ρ_G	gas phase density
ρ_L	liquid phase density
σ	surface tension
ψ	dimensionless gas phase superficial velocity

Subscripts

G	a gas phase quantity
L	a liquid phase quantity
meas	measured quantity
mix	mixture
pred	predicted quantity

Superscripts

DIERS	quantity used in the DIERS methodology

fractions. This is of interest as surface tension is an important parameter in the calculation of outflow conditions from a two-phase vessel undergoing level swell. In the context of a safety analysis of high pressure plant, an estimate of outflow provides source conditions for consequence models of fire and dispersion as well as providing a tool for estimating the time a vessel takes to blowdown following emergency depressurisation.

When top venting from a vessel in a two-phase state occurs, there is initially all vapour venting and the pressure drops. As the pressure falls, the liquid becomes increasingly superheated and bubbles form. This may cause level swell with the two-phase fluid vapour

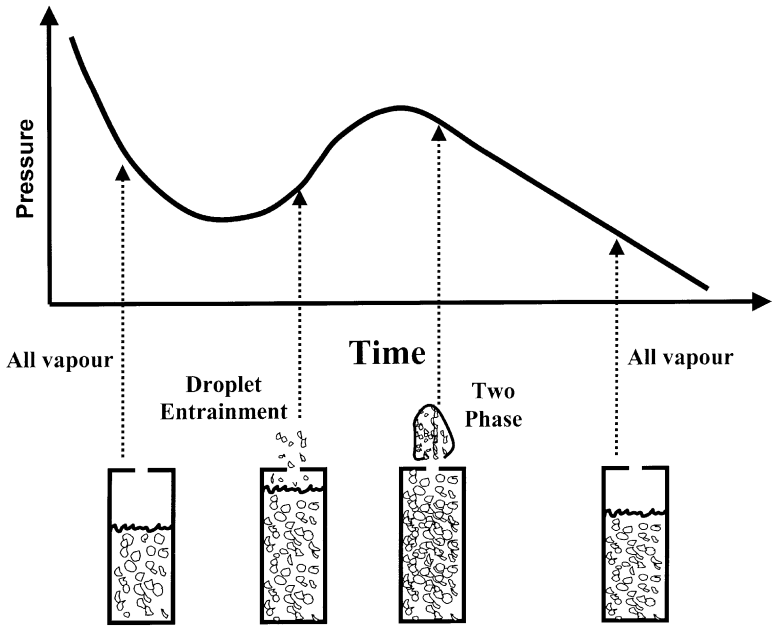

Fig. 1. Typical depressurisation behaviour of a top venting vessel undergoing level swell.

interface rising up the vessel. If the interface approaches within a certain critical distance of the vent, entrainment of liquid droplets into the vent may occur. If the interface reaches the vent, two-phase venting is likely, with the vessel pressure increasing. The rise in pressure occurs as the volumetric rate of flow through the vent reduces when two-phase venting occurs, whereas the vapour volume production from the superheated liquid is initially maintained. The pressure reaches a maximum and ultimately the interface falls below the vent entrance and all vapour venting prevails again. The process is illustrated schematically in Fig. 1.

The level swell model considered in later sections does not take into account, the time taken for the swell height to reach its maximum extent and assumes two-phase venting occurs instantaneously. This is acceptable as the initial rapid decrease and recovery in vessel pressure, occurs over a short time interval and adds little to the consequence assessment and tends to give conservative predictions of outflow early in the vessel depressurisation event. However, other studies have investigated the initial transient phase [1,2]. The models developed in [1,2] are not at a stage of development for general application as they include a number of parameters that must be estimated, such as the average bubble diameter.

The factors influencing the behaviour of the interface are: vessel shape and size, initial liquid height in the vessel, fluid composition and properties, vessel pressure, vapour production rate, vessel flow regime and vent size. In Section 2, the calculation of surface tension will be considered, as it is an important parameter in the estimation of level swell and two-phase outflow.

2. Calculation of surface tension

Methods for calculating surface tension can be divided into those requiring physical properties of the fluid such as the critical parameters [3], and those based on the chemical structure such as Sugden [4]. The physical property based methods tend not to be applicable to polar liquids without modification [3]. Sugden's method was further extended by Quale [5] and is known as the Macleod–Sugden correlation. The Macleod–Sugden correlation has the form

$$\sigma^{0.25} = [P](\rho_{\mathrm{L}} - \rho_{\mathrm{G}}) \tag{1}$$

where $[P]$ is the parachor. In most applications, the parachor can be taken to be constant with a negligible loss of accuracy, provided the operating conditions are remote from the critical point. Note that even as the pressure and temperature tend to the critical point that the Macleod–Sugden correlation for surface tension has the correct behaviour.

The Macleod–Sugden correlation has a typical error of less than 5%, although the error can be as large as 20% [3]. The Macleod–Sugden correlation also has the advantage over other surface tension calculation methods based on a corresponding states principle, such as Reidel's correlation [3], that it can be easily extended to mixtures

$$\sigma_{\mathrm{mix}}^{0.25} = \sum_{i=1}^{n} [P_i](x_i \rho_{\mathrm{L,mix}} - y_i \rho_{\mathrm{G,mix}})$$

where x_i and y_i denote the mole fraction of species i in the liquid and gas phases [3]. To calculate the surface tension, it remains to determine the parachor. Quale [5] tabulated values of the parachor for a number of chemical species. Alternatively, the parachor can be calculated by an additive structural group method. A table for a number of atomic groups can be found in Quale [5]. Beaton and Hewitt [6] have also presented the table in SI units. However, the compilation of Quale's is incomplete and the additive structural group method is not always applicable, as the contribution to the parachor for some atomic groups is not known. In addition, the molecular structure for the species of interest is not always known. A further consideration is that the additive structure group method is not easily implemented as part of a computer program. A method for calculating the parachor for hydrocarbons with little knowledge of the liquid properties is discussed below.

The starting point for the parachor prediction method is a method used in multiphase pipeline flow simulation [7], where the fluid composition is specified using petroleum fractions. Typically, the composition is defined as a number of petroleum fractions, where the boiling point and specific gravity of each fraction are known. The molecular weight could be known or inferred from the Kesler and Lee's correlation [8]. The first step is to calculate the hydrogen content of the fluid on a mass basis using the correlation of Hougen et al. [9]

$$M_{\mathrm{H}} = -0.1580 + 0.03157 \frac{T_{\mathrm{b}}^{1/3}}{\delta_{\mathrm{G}}} - 4.0046 \times 10^{-5}(T_{\mathrm{b}} - 225.02)$$

where the normal boiling point is given in Kelvin, and δ_{G} denotes the specific gravity. The

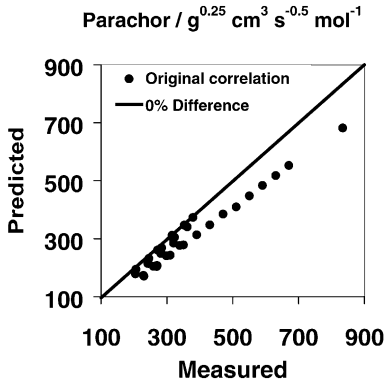

Fig. 2. Comparison of measured and predicted parachor calculated using Eq. (2).

atomicity can then be calculated

$$N = \left(\frac{M_{\mathrm{H}}}{1.0079} + \frac{1 - M_{\mathrm{H}}}{12.0111}\right) M_{\mathrm{w}}$$

and finally the parachor is approximated as

$$[P] = (21 - 65M_{\mathrm{H}})N \tag{2}$$

This expression for the parachor is given in [7]. Fig. 2 shows a comparison of Eq. (2) with the measured data taken from [5], for a range of fluids spanning the normal and iso-parafins, olefins, aromatics and napthenes, for species with a carbon atom count of up to 20.

There is a tendency for Eq. (2) to under predict the measured parachor. For the species considered, the mean error is just over 13% with a maximum error of just over 26%. This is not altogether satisfactory as the power law dependency between the parachor and surface tension, Eq. (1) implies that an under prediction of 26% in the parachor gives a 70% under prediction in the surface tension. The bias in the error suggests that the predictions could be significantly improved by introducing a correction term in Eq. (2). In Fig. 3 the ratio

$$\frac{[P]_{\mathrm{meas}}}{(21 - 65M_{\mathrm{H}})N}$$

is plotted against the abscissa, N/M_{w}. It can be seen that the species are grouped together on the basis of structure and there is a trend in the correction factor. Fitting a cubic polynomial to the data in Fig. 3 gives a correction factor for the original parachor Eq. (2) and the improved correlation,

$$[P] = (21 - 65M_{\mathrm{H}})N(2.3283 - 3.9546X + 4.1395X^2 - 1.4831X^3) \tag{3}$$

$$X = \frac{N}{M_{\mathrm{w}}} \quad 0.4 \leq X \leq 1.1$$

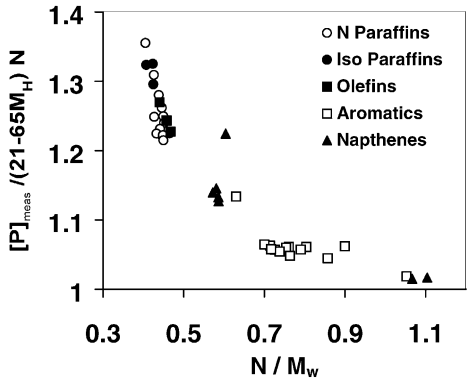

Fig. 3. Correction factor for the parachor Eq. (2).

For X greater than 1.1, the data in Fig. 3 suggest the original Eq. (2) is accurate. For X less than 0.4, the species are likely to be in a gaseous state at 15.6 °C (60 °F).

Fig. 4 shows a comparison of the new correlation with the measured parachor data of Quale [5]. The average error using Eq. (3) to approximate the parachor is just over 1%, whereas, the maximum error is less than 4%.

This improvement in parachor prediction has a significant influence on the surface tension prediction using the Macleod–Sugden method (Eq. (1)) because of the power law dependence between the parachor and surface tension. By way of example, the measured surface tension and the surface tension predicted using the Macleod–Sugden correlation using the measured parachor and the parachor calculated using Eq. (2) and the improved parachor Eq. (3) are shown in Fig. 5 for hexane. Hexane is used for illustrative purposes as the original parachor correlation, Eq. (2) predicted a particularly inaccurate estimate of the actual parachor for hexane. The differences in surface tension using the

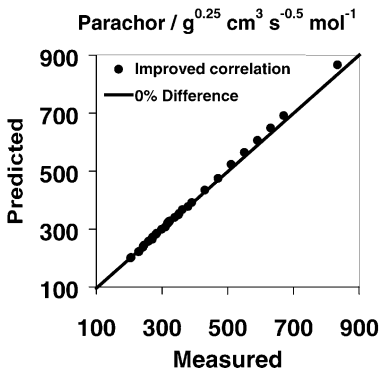

Fig. 4. Comparison of measured and predicted parachor calculated using the improved Eq. (3).

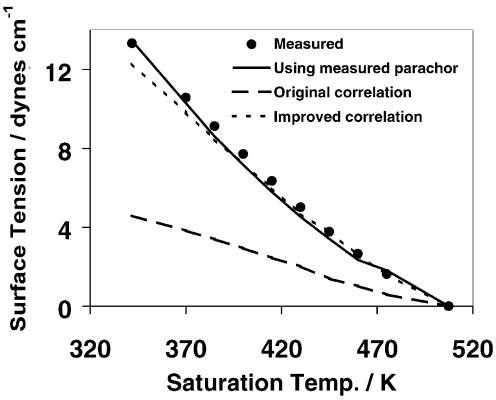

Fig. 5. Surface tension for hexane on the saturation curve.

different values of measured and predicted parachor are highlighted. The measured surface tension data are taken from [6]. As the surface tension tends to zero as the saturation temperature increases to the critical temperature, the mean relative error is taken as

$$\tilde{E}_{\mathrm{rel}} = \frac{\sum |\sigma_{\mathrm{meas}} - \sigma_{\mathrm{pred}}|}{\sum \sigma_{\mathrm{meas}}}$$

In this example, the agreement between the measured surface tension and the Macleod–Sugden correlation using the measured parachor is good, with a mean relative error of 5.6% in the surface tension prediction. The agreement between the measured surface tension and the Macleod–Sugden correlation using Eq. (3) to predict the parachor is also acceptable with a mean relative error of 6.3%. The predicted surface tension using Eq. (2) to calculate the parachor is significantly under predicted with a mean relative error of 63%. An error of this magnitude could have implications for the accuracy of any outflow prediction made using Eq. (2) to predict the parachor and in turn used to calculate the surface tension. In Section 3, some of the details of a methodology used to calculate outflow from a top-venting vessel will be described such that the sensitivity of outflow to the error in surface tension estimation can be assessed.

3. Level swell modelling

The level swell model described below follows the DIERS methodology, [10] with a number of improvements developed recently [11–13]. For brevity, the description of the level swell model will be restricted to a discussion of the elements of the model that differ from the DIERS methodology and surface tension is an important factor, for the churn turbulent flow regime. The methodology's extension to the bubbly flow regime requires only minor modifications.

The basis for estimating level swell is a drift flux model, [14], combined with a bubble rise velocity correlation. The bubble rise velocity correlation implemented is

$$U_{\text{bub}} = \begin{cases} 0.03\left[\dfrac{\sigma g(\rho_{\text{L}}-\rho_{\text{G}})}{\rho_{\text{L}}^2}\right]^{0.25}\left[\dfrac{\rho_{\text{G}}}{\rho_{\text{L}}}\right]^{-0.157} N_{\nu}^{-0.562}, & N_{\nu} \le 0.00225 \\ 0.92\left[\dfrac{\sigma g(\rho_{\text{L}}-\rho_{\text{G}})}{\rho_{\text{L}}^2}\right]^{0.25}\left[\dfrac{\rho_{\text{G}}}{\rho_{\text{L}}}\right]^{-0.157,} & 0.00225 < N_{\nu} \le 0.1 \end{cases} \tag{4}$$

$$N_{\nu} = \frac{\nu_{\text{L}}\rho_{\text{L}}}{\sqrt{\rho_{\text{L}}\sigma\sqrt{\frac{\sigma}{g(\rho_{\text{L}}-\rho_{\text{G}})}}}}$$

where σ is the surface tension and ν_{L} is the liquid phase kinematic viscosity. Wehmeier et al. [15] showed that this formation was a significant improvement over the equation

$$U_{\text{bub}}^{\text{DIERS}} = 1.53\left[\frac{\sigma g(\rho_{\text{L}}-\rho_{\text{G}})}{\rho_{\text{L}}^2}\right]^{0.25} \tag{5}$$

for correlating the gas phase mass flux in bubble columns. The DIERS superscript in Eq. (5) is introduced to indicate that this is the bubble rise velocity implemented in the DIERS methodology [10].

The bubble rise velocity influences the predicted vessel outflow in two ways. It is used to determine if two-phase venting is likely and it modifies the stagnation quality at the vent entrance as the flow in the vessel and at the entrance to the vent are coupled by imposing mass conservation between the vessel and the vent.

The above gives some insight into elements of the level swell model where the surface tension is required. A more detailed description of the level swell model can be found in [10–13].

4. Outflow sensitivity to surface tension prediction

4.1. Bubble rise velocity sensitivity

The bubble rise velocity sensitivity to the parachor is shown in Figs. 6 and 7, where the bubble rise velocity as a function of saturation temperature is plotted. Fig. 6 shows Wehmeier et al.'s [15] bubble rise velocity correlation on the saturation curve for hexane. Three curves are shown; the bubble rise velocity calculated using the measured parachor, the bubble rise velocity calculated using the parachor correlation Eq. (2) and the bubble rise velocity calculated using the parachor correlation Eq. (3). For convenience, the three curves in Fig. 6 are labelled as the 'accurate' bubble rise velocity curve, the 'original' parachor bubble rise velocity curve and the 'improved' parachor bubble rise velocity curve, respectively. The original parachor bubble rise velocity curve under predicts both the accurate and improved parachor bubble rise velocity curve. The improved bubble rise velocity curve also under predicts the

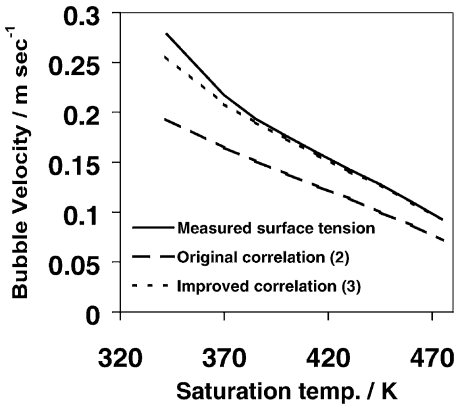

Fig. 6. Wehmeier et al.'s [15] bubble rise velocity correlation for hexane on the saturation curve.

accurate bubble rise velocity curve although the error is significantly less than for the original parachor bubble rise velocity curve. The margin of difference in Wehmeier et al.'s [15] bubble rise velocity is less than that exhibited in the surface tension comparisons because the bubble rise velocity correlation has a power law dependency on the surface tension

$$U_{\text{bub}} = \begin{cases} O(\sigma^{0.67}) = O([P]^{2.7}) & N_v \leq 0.00225 \\ O(\sigma^{0.25}) = O([P]) & 0.00225 < N_v \leq 0.1 \end{cases}$$

In the predicted bubble rise velocity shown in Fig. 6, the parameter N_v exceeds 0.00225 so the fourth root dependency on surface tension translates into a linear dependence on parachor. Similar trends are exhibited in Fig. 7 for the DIERS bubble rise velocity, as the dependence on parachor is linear.

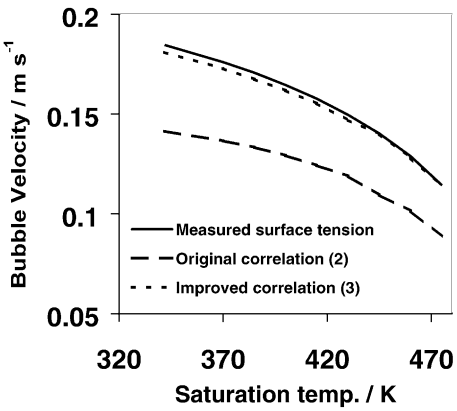

Fig. 7. DIERS bubble rise velocity correlation [10], for hexane on the saturation curve.

5. Outflow and level swell sensitivity

The sensitivity of the outflow model to surface tension is considered further below by considering outflow from a hypothetical vessel processing pentane. Pentane was chosen as the parachor correlation in Eq. (2) exhibits the largest error (26%) of the chemical species considered. Therefore, outflow from a vessel processing pentane has the most sensitivity to the method of estimating the parachor. The vessel has a volume of 10 m^3 and a diameter of 3 m. The operating conditions of the vessel are taken to be a saturation pressure of 10 bar and an initial void fraction of 0.02. The vent is modelled as an orifice with a diameter of 30 mm and a discharge coefficient of 0.8. The basis of the vessel outflow model and its validation has been described previously [11,16]. The model consists of a system of ordinary differential equations describing mass and energy balances for the vessel. Two-phase outflow is modelled using the homogeneous equilibrium assumption, coupled to the level swell model described above. The homogeneous equilibrium two-phase vent model, [10], is accurate for the flow of hydrocarbons through orifices [16,17]. When the level swell model predicts gas phase venting the vent model used is based on the isentropic nozzle flow equations [18]. Apart from some of the features discussed above and those considered in, [11–13,16] the model is similar to the vessel depressurisation model SAFIRE [19] and will not be described in more detail.

Fig. 8 shows a comparison of the predicted mass flow rate and static vapour quality at the orifice throat. Three predictions are shown, one using the measured parachor, a second using Eq. (2) to estimate the parachor and the final curve calculated using Eq. (3) to estimate the parachor. For convenience the three simulations are labelled as the ‘accurate’ simulation, the ‘original’ parachor simulation and the ‘improved’ parachor simulation, respectively. In Fig. 8a, predictions of static vapour quality are shown. The predicted static vapour quality calculated in the original parachor simulation indicates two-phase venting stops approximately 140 s after vessel depressurisation begins, whereas the static vapour quality prediction calculated in the accurate parachor simulation indicates two-phase venting stops after approximately 50 s. The time taken for two-phase venting to end in the improved parachor simulation is approximately 60 s.

Considering the mass flow rate predictions in Fig. 8b, the relative difference in predicted mass flow rate between the accurate simulation and the original parachor simulation is of the order of 5–10% in the first 50 s of the vessel depressurisation event. After 50 s, the relative difference in mass flow rate increases to 30–35% as two-phase venting has ended in the accurate simulation but continues in the original parachor simulation. Comparing the mass flow rate calculated in the accurate parachor simulation and the improved parachor simulation, the two predictions are in close agreement, having a typical relative error of 1% except between 50 and 60 s where the phase of the release differs. In the 50–60 s time interval, the relative difference between the mass flow rates calculated in the accurate simulation and the improved parachor simulation is of the order of 20%.

The vessel pressure calculated using the measured parachor and the original parachor correlation is shown in Fig. 9. The vessel pressure calculated using the improved parachor correlation is not shown, as it is indistinguishable from the curve calculated using the measured parachor. The difference in vessel pressure during the early stages of the vessel depressurisation simulations is small up to a time of approximately 80 s after which the

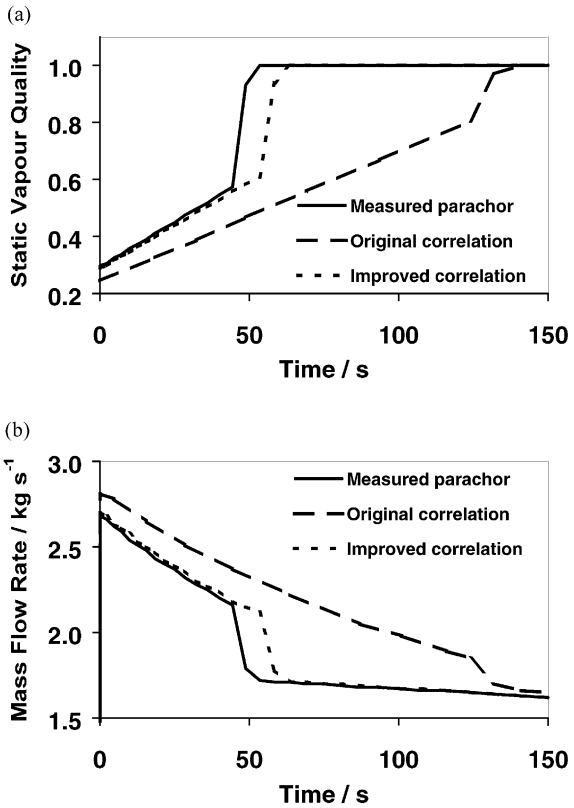

Fig. 8. Outflow predictions for a vessel processing saturated pentane: (a) static vapour quality and (b) mass flow rate.

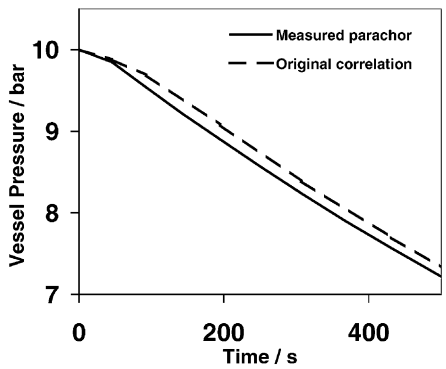

Fig. 9. Predicted pressure for a vessel venting pentane.

vessel pressure calculated using the original parachor correlation over predicts the curve calculated using the measured parachor. The maximum relative difference between the two vessel pressure curves is of the order of 2%, a much smaller margin than exhibited in the mass flow rate predictions. The sensitivity of the mass flow rate to the parachor is due to its influence on the phase of the release, principally the duration of two-phase venting. The insensitivity of the vessel pressure predictions to the value of the parachor is because the time interval over which the release phase is different for the vessel simulations is small relative to the time-scale over which the vessel depressurisation occurs.

This suggests the time taken for a vessel to depressurise is not sensitive to the method used to estimate the parachor. Whereas, the outflow rate early on in a vessel failure incident, when it is most critical to estimating the consequences of a release is sensitive to the value of the parachor used.

6. Conclusion

An improved correlation for the parachor has been presented. The improved parachor correlation requires knowledge of the normal boiling point and the specific gravity, consistent with the specification of composition by petroleum fractions. The new correlation has a typical error of the order of 1% for the species considered compared to a typical error of 13% for the original correlation. The sensitivity of physical parameters to changes in the parachor, such as the surface tension has been considered. The fourth power dependence of the surface tension on the parachor shows that the parachor must be as accurately estimated as possible if significant errors in the surface tension are to be avoided.

In the context of vessel depressurisation simulation, a methodology for predicting level swell behaviour similar to the DIERS methodology [10] has been analysed and found to depend on the surface tension via the bubble rise velocity correlation. Changes in the bubble rise velocity effect the predicted stagnation quality at the vessel vent. Overall the sensitivity of vessel outflow prediction to surface tension if the parachor is under predicted is such that, the time interval that two-phase venting occurs can be over predicted by 2–3 times, the time interval compared to where the parachor is accurately estimated. This has an impact on the error in the mass flow rate prediction, which if used as a source condition for other consequence models would propagate throughout the consequence analysis. This could also have implications for vent sizing calculations.

Acknowledgements

The author acknowledges Dr J. Wilday and Professor B Boesmans for their constructive and thorough reviews, which have significantly improved the paper.

References

[1] B. Boesmans, J. Berghmans, Modelling boiling delay and transient level swell during emergency pressure relief of liquefied gases, J. Hazardous Mat. 46 (1996) 93–104.

[2] H.J. Viecenz, Rise of bubbles and phase separation in vessels during vapour introduction and depressurisation, Ph.D. Thesis, University of Hanover, 1980.
[3] R.C. Reid, J.M., Prausnitz, B.E. Poling, The Properties of Gases and Liquids, 4th Edition McGraw-Hill, New York, 1987.
[4] S. Sugden, A relation between surface tension, density, and chemical composition, J. Chem. Soc. 125 (1924) 1177–1189.
[5] O.R. Quale, The parachors of organic compounds, Chem. Rev. 53 (1953) 439–585.
[6] C.F. Beaton, G.F. Hewitt, Physical property data for the design engineer, Hemisphere, New York, 1989.
[7] Pipeline Analysis Code (PLAC), Technical Manual 5.2, AEA Technology, 1994.
[8] M.G. Kesler, B.I. Lee, Improve prediction of enthalpy of fractions, Hydrocarbon Processing 55 (3) (1976) 153–162.
[9] A.O., Hougen, K.M. Watson, R.A. Ragatz, Chemical Process Principles, Part 1, 2nd Edition, Wiley, New York, 1954.
[10] Draft DIERS Technology Report, Emergency Relief Systems for Runaway Chemical Reactions and Storage Vessels: a Summary of Multiphase Flow Methods, Fauske and Associates, IL, USA, 1984.
[11] P.S. Cumber, Modelling top venting vessels undergoing level swell, J. Hazardous Mat. 89 (2002) 109–125.
[12] C.M. Sheppard, Drift-flux correlation disengagement models, Part II, Shape based correlations for disengagement prediction via churn–turbulent drift-flux correlation, J. Hazardous Mat. 44 (1995) 127–139.
[13] C.M. Sheppard, S.D. Morris, Drift-flux correlation disengagement models, Part I, Theory: analytic and numeric integration details, J. Hazardous Mat. 44 (1995) 111–125.
[14] G.B. Wallis, One-dimensional two-phase flow, McGraw-Hill, New York, 1969.
[15] G. Wehmeier, F. Westphal, L. Friedel, Pressure relief system design for vapour or two-phase flow: process safety and environmental protection, Trans. IChemE B 72 (1994) 142–148.
[16] P.S. Cumber, Modelling outflow from high pressure vessels: Process Safety and Environmental Protection, Trans. IChemE B 79 (2001) 13–22.
[17] Guidelines for the safe and optimum design of hydrocarbon pressure relief and blowdown systems, Institute of Petroleum 2001.
[18] A.H. Shapiro, The Dynamics and Thermodynamics of Compressible Fluid Flow, Wiley, New York, 1953.
[19] A.N. Skouloudis, Benchmark exercises on the emergency venting of vessels, J. Loss Prevention Process Industries 5 (1992) 89–103.